

# A Recurrent *ADPRHL1* Germline Mutation Activates PARP1 and Confers Prostate Cancer Risk in African American Families

Guanyi Zhang<sup>1</sup>, Zemin Wang<sup>1</sup>, Jasmin Bavarva<sup>1</sup>, Katherine J. Kuhns<sup>1</sup>, Jianhui Guo<sup>1</sup>, Elisa M. Ledet<sup>2</sup>, Chiping Qian<sup>1</sup>, Yuan Lin<sup>1</sup>, Zhide Fang<sup>3</sup>, Jovanny Zabaleta<sup>4</sup>, Luis Del Valle<sup>5</sup>, Jennifer J. Hu<sup>6</sup>, Diptasri Mandal<sup>2</sup>, and Wanguo Liu<sup>1,2</sup>



## ABSTRACT

African American (AA) families have the highest risk of prostate cancer. However, the genetic factors contributing to prostate cancer susceptibility in AA families remain poorly understood. We performed whole-exome sequencing of one affected and one unaffected brother in an AA family with hereditary prostate cancer. The novel non-synonymous variants discovered only in the affected individuals were further analyzed in all affected and unaffected men in 20 AA-PC families. Here, we report one rare recurrent *ADPRHL1* germline mutation (*c.A233T*; *p.D78V*) in four of the 20 families affected by prostate cancer. The mutation co-segregates with prostate cancer in two families and presents in two affected men in the other two families, but was absent in 170 unrelated healthy AA men. Functional characterization of the mutation in benign prostate cells showed aberrant promotion of cell proliferation, whereas expression of the wild-type *ADPRHL1* in prostate cancer cells suppressed cell proliferation and oncogenesis. Mechanistically, the

*ADPRHL1* mutant activates PARP1, leading to an increased H<sub>2</sub>O<sub>2</sub> or cisplatin-induced DNA damage response for prostate cancer cell survival. Indeed, the PARP1 inhibitor, olaparib, suppresses prostate cancer cell survival induced by mutant *ADPRHL1*. Given that the expression levels of *ADPRHL1* are significantly high in normal prostate tissues and reduce stepwise as Gleason scores increase in tumors, our findings provide genetic, biochemical, and clinicopathological evidence that *ADPRHL1* is a tumor suppressor in prostate tissue. A loss of function mutation in *ADPRHL1* induces prostate tumorigenesis and confers prostate cancer susceptibility in high-risk AA families.

**Implications:** This study highlights a potential strategy for *ADPRHL1* mutation detection in prostate cancer–risk assessment and a potential therapeutic application for individuals with prostate cancer in AA families.

## Introduction

Prostate cancer is the most prevalent cancer in men and the second leading cause of cancer-related death worldwide (1). Previous studies have reported that prostate cancer is the most inherited cancer type among all types of solid tumors (2, 3). About 20% of men diagnosed with prostate cancer have a positive family history and up to 10% of total prostate cancer cases are hereditary (4–6). However, the genetic components conferring prostate cancer susceptibility in the individuals with hereditary prostate cancer are largely unknown. Because family history of

prostate cancer is a well-recognized risk factor, and African American (AA) men have the highest incidence of prostate cancer among all ethnic groups (7), whole-genome sequencing (WGS) analysis of high-risk AA-PC families would facilitate identification of genetic factors that contribute to prostate cancer susceptibility. Although recent studies using WGS technologies on AA-PC individuals are increasing, very limited high-risk susceptibility genes have been identified (8–11). Studies using the same technologies on hereditary AA-PC families for identification of high-risk genes remain lacking.

In this study, we focused on genomic and genetic analyses of 20 hereditary AA-PC families through initial whole-exome sequencing (WES) of blood DNA from one affected and the eldest unaffected brother in a hereditary AA-PC family to identify potential genetic risk factors. The rare non-synonymous variants identified only in the affected individuals from this family were further evaluated in 19 other high-risk AA-PC families and were compared with publicly available databases and publications. One recurrent germline mutation (*c.A233T*; *p.D78V*) in the *ADPRHL1* gene (also known as *ARH2*; ADP-Ribosylhydrolase Like 1) was identified in four families. We performed biochemical and clinicopathological analyses of this mutation and exploited its potential roles and mechanisms in AA-PC susceptibility and tumorigenesis. Our data, presented here, indicate that *ADPRHL1* is a tumor suppressor and a mutation in the *ADPRHL1* gene increases susceptibility and oncogenesis in the prostate. Thus, the *ADPRHL1*-mediated signaling pathway is a potent potential therapeutic target of prostate cancer.

<sup>1</sup>Stanley S. Scott Cancer Center, Louisiana State University Health Sciences Center, New Orleans, Louisiana. <sup>2</sup>Department of Genetics, School of Medicine, Louisiana State University, New Orleans, Louisiana. <sup>3</sup>Biostatistics, School of Public Health, Louisiana State University Health Sciences Center, New Orleans, Louisiana. <sup>4</sup>Department of Interdisciplinary Oncology, Stanley S. Scott Cancer Center, Louisiana State University Health Sciences Center, New Orleans, Louisiana. <sup>5</sup>Department of Pathology, Louisiana State University Health Sciences Center, Louisiana Cancer Research Center, New Orleans, Louisiana. <sup>6</sup>Sylvester Comprehensive Cancer Center, University of Miami, Miller School of Medicine, Miami, Florida.

**Corresponding Author:** Wanguo Liu, Louisiana State University Health Sciences Center, New Orleans, LA 70112. Phone: 504-210-3326; Fax: 504-210-2279; E-mail: wliu2@lsuhsc.edu

Mol Cancer Res 2022;20:1776–84

doi: 10.1158/1541-7786.MCR-21-0874

©2022 American Association for Cancer Research

## Materials and Methods

### Study Subjects and Tissue Specimens

Twenty AA high-risk prostate cancer families included in this study were primarily recruited from 12 Louisiana parishes with cases distributed throughout Southeastern and South Central Louisiana as previously described (12, 13). The group of 95 healthy AA men (over age 60) was collected by Dr. J.J. Hu as previously described (14). Seventy-five AA men (ages 45–82) without any cancer and 17 pairs of anonymous snap-frozen prostate tumors from AA men and their matched adjacent normal prostate tissues were obtained from the Biospecimen Core of the Louisiana Cancer Research Consortium (LCRC) as previously described (15). Two experienced pathologists evaluated histological classification, including Gleason score and tumor cell content. The prostate tissue microarray (Catalog #PR807b) was purchased from US Biomax. This study was approved by the Institutional Review Board of Louisiana State University Health Sciences Center in New Orleans.

### WES

We performed WES in the genome center in Louisiana State University Health Sciences Center in New Orleans as previously described (16). Briefly, 1- $\mu$ g genomic DNA isolated from one affected or one unaffected brother in AA-PC family #134 was sheared, size selected, ligated to sequencing adapters, and PCR amplified following standard library preparation, respectively. The post-PCR libraries were then used for exome capture using the Agilent SureSelect Human All Exon v4 Capture Kit. Exome enriched samples were sequenced using 2 ( $2 \times 75$  bp) lanes on an Illumina HiSeq 2000 (Illumina, Inc.).

### Analyses of WES data

The sequence reads passing Illumina chastity filter were subjected to a quality filter step that removed low-quality bases and were aligned to the human genome (hg18) using Maq19 and BWA20 software (17). The percentage alignment of the reads for the reference genome and the targeted region, exome, was calculated using Perl scripts (18). Our reads covered 80.8% of the targeted region with over 25-fold coverage. Sequence calls for single-nucleotide polymorphisms (SNP) and insertions and deletions (indels) were performed using the GATK (Broad's Genome Analysis Toolkit, v2.1–8-g5efb575). The indels were detected on the reads aligned with BWA for its ability to allow for gaps during the alignment (17). Shared homozygous segments of the affected individuals were detected using Plink software version 1.06 (19). Only non-synonymous changes (SNPs and indels), splice site variants, and/or an aberrant stop codon changes were considered for further analysis. The variants were annotated for novelty compared with both dbSNP (build 130) and available genome databases, including 1,000 genomes and gnomAD. Variants located outside of coding regions or with frequencies  $>1\%$  were excluded. All insertion and deletion variants were considered damaging, whereas the damaging of the SNP variants on their encoded protein were evaluated using algorithms of Sorting Intolerant from Tolerant (SIFT) and PolyPhen-2 (Polymorphism Phenotyping v2; ref. 20). After these steps, we identified 225 novel ns-variants that damage protein function (Supplementary Table S1).

### Sanger sequencing

All 225 non-synonymous *ADPRHL1* variants identified by WES in the discovery phase were confirmed by Sanger sequencing. We also performed Sanger sequencing of the 14 mutations that co-segregated

with the prostate cancer phenotype in AA-PC family #134, in all affected and unaffected men in an additional 19 AA-PC families and 170 healthy AA men to define which one of the mutations confers increased risk to prostate cancer in AA-PC families. We also performed Sanger sequencing of the promoter regions, exons, and exon flanking regions of *ADPRHL1* for other potential mutations in all affected men in the 20 AA-PC families. Sequencing reactions were performed using the BigDye Terminator V3.1 Cycle Sequencing kit (Life Technologies) according to the manufacturer's protocol. Sequencing products were analyzed on the ABI Prism 3500XL Genetic Analyzer (Life Technologies). All sequences were compared with the *ADPRHL1* RefSeq sequence for variant detection using Mutation Surveyor software (Software SofeGenetics).

### Plasmids and mutagenesis

We carried out site-directed mutagenesis (Agilent Technologies) to generate different mutation constructs of *ADPRHL1* by PCR amplified the *ADPRHL1* C182G and A233T cDNAs from *ADPRHL1* wild-type construct, and cloned the PCR amplicons separately into a TA-cloning vector (Promega). Fusion constructs of *ADPRHL1* C182G and C233T with FLAG tag were generated by subcloning the cDNAs from the TA-plasmids into the BamHI and XhoI sites of the pCMV 2b vectors. All plasmids were sequence verified.

### Cell proliferation and anchorage-independent growth assays

Cells were plated at a density of  $2 \times 10^5$  cells per well in 6-cm dishes and were trypsinized at days 2, 4, and 6 and counted using a hemocytometer after stained with trypan blue. Clonogenic growth of cells was evaluated by assessing plating efficiency for anchorage-independent growth in soft agar at day 16 after plating, as previously described (15).

### Immunoprecipitation and immunoblotting

Immunoblotting and immunoprecipitation (IP) were performed using various antibodies as described previously (15). The antibodies used in this study are PARP1,  $\gamma$ -H2A.X, *ADPRHL1* and  $\beta$ -actin (Cell Signaling Technology Cat#9532, Cat#9718, Santa Cruz Biotechnology sc-93978, and Sigma A2228). The following are the IP experiments performed: Cells were lysed in the lysis buffer described above and pre-clearing was performed by two consecutive incubations with protein G-Sepharose at 4°C for 30 minutes. Binding to specific Abs was performed by incubation at 4°C for 4 hours, followed by incubation with protein G-Sepharose at 4°C for 1 hour. After six washes with lysis buffer, immunocomplexes were eluted with 100 mmol/L glycine pH 2.5, followed by pH neutralization using Tris to a final concentration of 50 mmol/L. The immunocomplexes were then separated by SDS-PAGE (21).

### IHC and immunofluorescence analyses

IHC analysis of the human tissue microarray was conducted using *ADPRHL1* antibody (Santa Cruz Biotechnology sc-93978) in Molecular Histopathology and Analytical Microscopy Core (MHAM) as previously described (15). For immunofluorescence analysis, cells were transfected with indicated plasmids on poly-D-Lysine-coated cover-glasses (neuVibro) and cultured in RPMI-1640 complete medium supplemented with 10% FBS. At 48 hour after transfection, cells were fixed with 4% paraformaldehyde, and incubated with a pan-AR antibody (PG-21, Millipore; 1:200) overnight at 4°C and subsequently with Alexa Fluor 488-conjugated secondary antibody (Invitrogen; 1:1,000) for 1 hour at room temperature in the dark. Nuclei were then stained with 4', 6-diamidino-2-phenylindole. Confocal images

were obtained by using a Leica TCS SP2 system with a 40× oil-immersion objective on a Z-stage (22).

### Statistical analysis

Results of *in vitro* experiments were presented as standard deviation or standard error. The student *t* test was used to compare continuous variables when there were two groups. The Exact Binomial test was applied for proportion comparison. Exact confidence interval was provided for odds ratio. Pairwise comparisons were made using ANOVA within the models at cross-sections and the Bonferroni multiple comparisons adjustment was used for pairwise tests. Analyses were completed using SAS 9.4 (SAS Institute). The mean values between prostates groups were compared in ANOVA by Tukey's multiple comparisons using GraphPad Prism 6.0 (GraphPad Software, Inc.). Alpha of 0.05 determined statistical significance (23).

### Data availability statement

The human sequence data generated in this study are not publicly available due to complying with patient privacy requirements stated in the consent forms collected during enrollment. The study participants were consented to the implementation of data sharing requirements and no permission was obtained about depositing genomic data in the public repository database. The data will be available from the corresponding author upon reasonable request. Other data generated in this study are available within the article and its Supplementary Data Files.

## Results

### Identification of ADPRHL1 mutations in AA-PC families

To identify gene mutations in high-risk AA-PC families, we first performed WES on germline DNA from the youngest affected man (56-years-old) and the eldest unaffected brother (82-years-old) in a high-risk AA-PC family with six affected blood relatives (#134; Fig. 1). Bioinformatics analysis of the WES data by removing synonymous and common non-synonymous variants identified 225 rare non-synonymous variants present in the affected, but absent in the unaffected brother of this family (Supplementary Table S1). Sequencing analysis of the 225 variants in five affected and three unaffected men of this family (age >50) defined 14 rare non-synonymous variants segregating with the prostate cancer phenotype (Table 1). The criteria for considering co-segregation were defined as the mutation to be present in at least 3 affected brothers and absent in at least 3/4 unaffected brothers in the family, due to genetic heterogeneity of this disease.

Subsequent analyses of the 14 variants in an additional 19 unrelated AA-PC families consisting of 53 affected and 52 unaffected men identified a novel *ADPRHL1* heterozygous missense mutation (*c.A233T*; *p.D78V*) in four out of 20 AA-PC families. Other variants were excluded as disease affected mutations, because they were either present in both affected and unaffected men, they did not co-segregate with prostate cancer in more than one AA-PC families, or they presented in the general AA population with frequencies of over 1% in the publicly available database.

This *ADPRHL1 c.A233T* mutation co-segregated with prostate cancer among the men in two of the four families. In family #134, all three affected brothers were carriers of the mutation, but none of all four unaffected brothers was. In family #3, both affected brothers were carriers of the mutation. In the remaining two families, only probands were available for analysis and both were carriers of this mutation

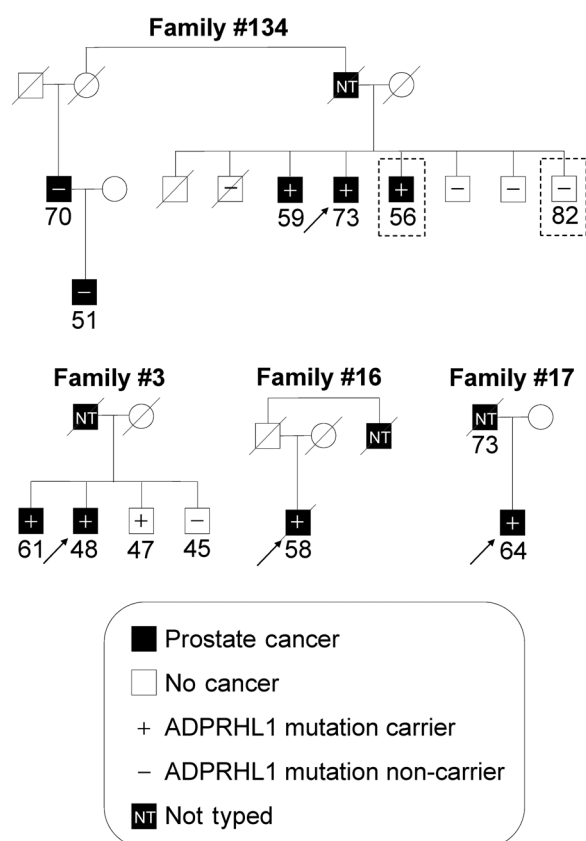


**Figure 1.**

Pedigrees of four AA-PC families carrying *ADPRHL1* mutations. The initial WES analysis of one affected and one unaffected brothers in AA-PC family #134 are highlighted. The proband in each pedigree is indicated by the arrow. Other symbols used in pedigrees are described previously in the key. Squares indicate male sex, and circles female sex. Ages of subjects are shown under the symbols. A slash through the symbol indicates that the subject is deceased.

(Fig. 1A). Subsequent sequencing analyses of all exons of the *ADPRHL1* gene in the affected and unaffected men of the remaining 16 AA-PC families did not identify any other *ADPRHL1* non-synonymous variants.

To determine the frequency of the *ADPRHL1* gene mutation in the general AA population, we sequenced the *ADPRHL1* gene in 170 healthy AA men between 45 and 82-years-old. We did not detect any of the non-synonymous variants with the exception of the *c.T182C* polymorphism. However, it is intriguing that the frequency of the *c.A233T* mutation in gnomAD database is about 0.8% in AA population ([https://gnomad.broadinstitute.org/variant/13-114098886-T-A?dataset=gnomad\\_r2\\_1](https://gnomad.broadinstitute.org/variant/13-114098886-T-A?dataset=gnomad_r2_1)). Because the *c.A233T* mutation is present 7/9 affected individuals in 4/20 prostate cancer families studied, it represents 20% carrier frequency in our high-risk AA-PC family cohort. Thus, the frequency of this mutation in AA-PC families is about 25-fold higher than in the general AA population ( $P = 0.000018$ ). Comparing with the 170 controls, the odds ratio is 93, with the lower endpoint of the exact 95% one-sided confidence interval being 8.55. These data suggest that the germline *ADPRHL1 c.A233T* mutation is a genetic risk factor for prostate cancer in the hereditary AA-PC families.

**Table 1.** Segregation analysis of the 14 novel ns-variants in AA-PC family #134.

Gene Symbols	2-5	2-6	2-9	1-10	2-10	2-19	2-11	2-20	2-12	Mutation classes	Chr. region	Function
SEZ6L										Missense	17q11.2	Cholesterol regulation
HPS4										Missense	22q12.1	Lysosome biogenesis
ZNF418										Missense	19q13.4	Inhibit MAPK signaling
PRAMEF1										Missense	1p36.21	Regulation of TRAIL
HSD17B2										Missense	16q23.3	Sex steroid biosynthesis
C10orf11										Frameshift	10q22.2	Albinism-causing gene
TRPM1										Missense	15q13.3	Cation Channel M
ADPRHL1										Missense	13q34	Altered in breast cancer
DCDC2										Missense	6p22.1	TSG in liver cancer
MYO16										Splicing	13q33.3	Schizophrenia gene
AKRIC3										Nonsense	10p15.1	Cullin-ligase substrate
GCNT2										Missense	6p24.3	Glycol-metabolism
SNX31										Missense	8q22.3	Mutated in melanoma
LIP1										Missense	21q11.2	Fats breakdown

Note: Individuals 1-10 and 2-5 to 2-10 are affected and individuals 2-11 to 2-20 are unaffected in family #134. Filled box indicates the individual carrying the mutation and unfilled box indicates the individual carrying no mutation.

### ADPRHL1 c.A233T mutation induces prostate cancer cell proliferation and oncogenesis

To explore the potential pathological impacts of this mutation in prostate cancer susceptibility and tumorigenesis, we expressed wild-type ADPRHL1 (ARH2-WT) in the AA-PC cell line (MDA PCa 2b) or the CA-PC cell line (C4-2B). We found that the growth rate of cancer cells expressing ARH2-WT were significantly reduced as compared with the control cells expressing the empty vector or the ADPRHL1 c.A233T mutant (ARH2-Mut; **Fig. 2A**). Consistently, in the colony formation assay, the cancer cells expressing ARH2-WT formed significantly lower numbers of colonies than those of the control cells (**Fig. 2B**). Moreover, in the anchorage-independent soft agar assays, the cells expressing ARH2-WT more greatly suppressed foci formation in comparison with the control cells, whereas the cells expressing ARH2-Mut lost the suppressive function as ARH2-WT shown by generating almost the same size and numbers of foci as the control cells (**Fig. 2C**). In contrast, in the benign prostate BPH-1 or P69 cells, expression of the ARH2-Mut increased cell proliferation rate and colony formation ability (**Fig. 2D** and **E**). These data indicate that ARH2-WT is required for suppression of prostate cancer cell proliferation and oncogenesis, and the c.A233T mutation in ADPRHL1 causes loss of its suppressive function. This evidence further suggests that ADPRHL1 is a potent tumor-suppressor gene in prostate cancer.

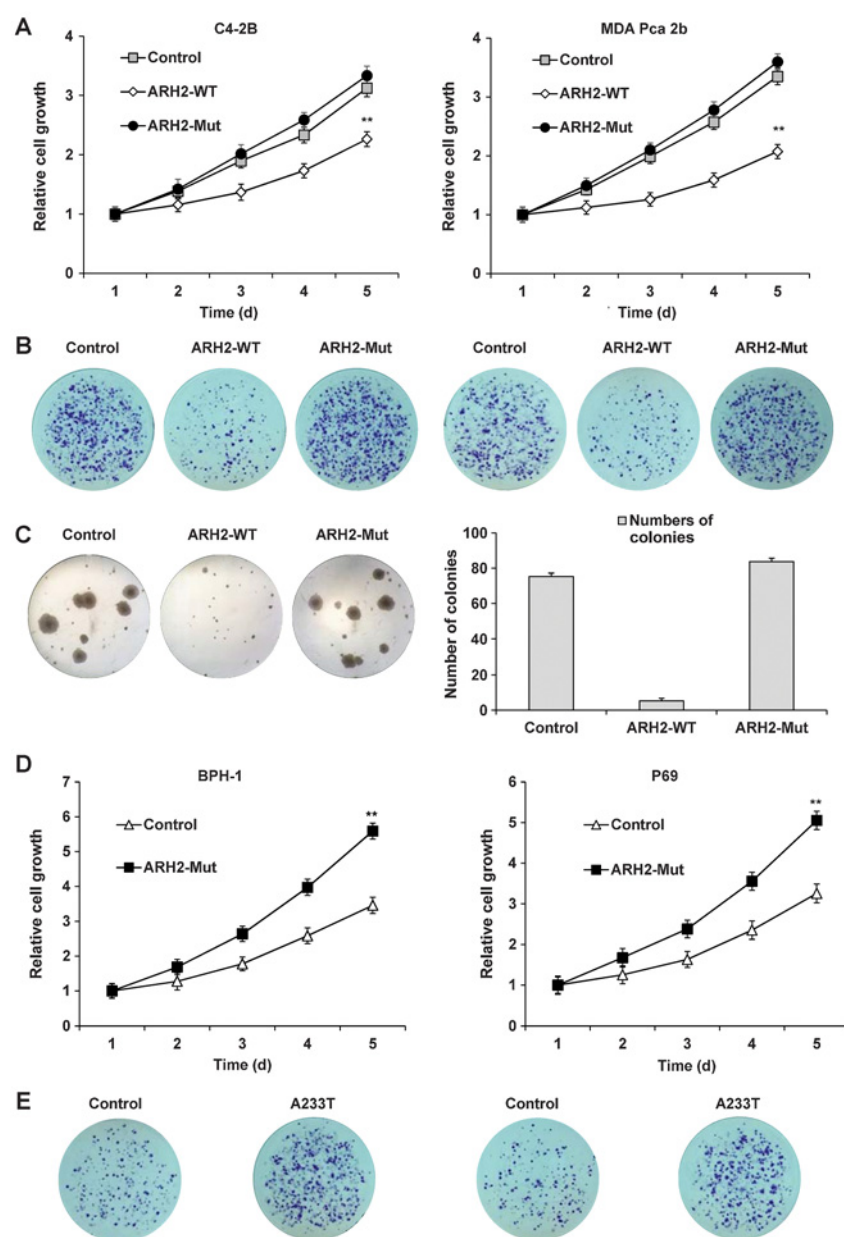
### ADPRHL1 c.A233T mutation activates PARP1 for prostate cancer cell survival

Because previous reports indicated that ARH3, a family member of ADPRHL1 (also known as ARH2), regulated PARP1 activity in various cancers (24, 25), we investigated the capability of ADPRHL1 in regulation of PARP1 in prostate cancer cells. We expressed ARH2-WT or the ARH2-Mut (ADPRHL1 c.A233T mutant) in MDA PCa 2b cells. To determine that ADPRHL1 c.A233T is not a polymorphism, we included the ADPRHL1 c.T182C polymorphism (over 5% in AA general population) in this analysis. We found that the cells expressing ARH2-Mut, but not ARH2-WT, or the T182C polymorphism, increased PARP1 activity as indicated by increased PAR levels by Western blotting (**Fig. 3A**). Consistently, immunofluorescence analysis confirmed the above results by showing increased levels of nuclear PAR in ARH2-Mut-expressing cells, as compared with the cells expressing ARH2-WT or the T182C polymorphism (**Fig. 3B**).

Because PARP1 participates in the DNA damage response (DDR) to prevent double-stranded DNA breaks (26, 27), we analyzed the MDA PCa 2b cells expressing ARH2-WT or ARH2-Mut for DNA damage following treatment with H<sub>2</sub>O<sub>2</sub>. We found that H<sub>2</sub>O<sub>2</sub> induced DNA damage equally in both cell types via resulting equivalent levels of  $\gamma$ -H2A.X (**Fig. 3C**). However, the PARP1 level was significantly increased in cells expressing ARH2-Mut as compared with those expressing ARH2-WT, indicating that ARH2-Mut increases PARP1 level to response to H<sub>2</sub>O<sub>2</sub>-induced DNA damage in prostate cancer cells (**Fig. 3C**). In agreement, under H<sub>2</sub>O<sub>2</sub>-induced DNA damage, the viability of the cells expressing ARH2-Mut also significantly increased compared with that of the cells expressing ARH2-WT (**Fig. 3D**). However, the same cells treated with PARP1 inhibitor (olaparib) diminished the viability of the ARH2-Mut-expressing cells, suggesting that ARH2-Mut-mediated cell survival occurs via PARP1-mediated DDR (**Fig. 3D**). These results were replicated in the same cells exposed to cisplatin or in the AA-PC-specific C4-2B cells exposed to either H<sub>2</sub>O<sub>2</sub> or cisplatin (Supplementary Fig. S1). Together, these data indicate that ADPRHL1 is required for suppressing the PARP1-mediated DDR and that the ADPRHL1 c.A233T mutation activates PARP1 to enhance DDR for prostate cancer cell survival.

### ADPRHL1 is downregulated in prostate cancer

To determine the clinical relevance of ADPRHL1, we determined the expression levels of ADPRHL1 in 17 pairs of prostate tumors and their matched normal biopsies (10 AA- and 7 CA-PC) by using Western blot. Except pair #14, in which ADPRHL1 was not detectable in both tumor and its matched normal, we observed a reduction of ADPRHL1 levels in 15 of 16 prostate tumors as compared with their matched adjacent normal prostate tissues (**Fig. 4A**). The ADPRHL1 levels in the majority of normal tissues were more than 3 times those in the matched tumor tissues (**Fig. 4B**). We further performed IHC analysis of a prostate tissue microarray containing 80 unrelated prostate tissue specimens with ADPRHL1 antibody. **Fig. 4C** shows the representative images of ADPRHL1 IHC staining from normal prostate tissues through Gleason 10 prostate adenocarcinomas. Interestingly, we observed significantly high levels of ADPRHL1 in 97% (29/30) of prostatic normal or hyperplasia tissues, mild to weak levels in 90% (27/30) of prostate tumor tissues with Gleason scores of 4-7, and very weak or

**Figure 2.**

ARH2-WT but not ARH2-Mut inhibits prostate cancer cell growth and oncogenesis. **A**, The growth rate of ARH2-WT-transfected cells was slower than that of vector or ARH2-Mut transfected MDA Pca 2b or C4-2B cells in the MTT assay ( $P < 0.005$ ;  $t$  test). Values represent mean  $\pm$  SD of three independent experiments performed in triplicate in all experiments. **B**, The numbers of colonies in ARH2-WT transfected cells were significantly lower than that of vector or ARH2-Mut transfected cells in colony formation assay. **C**, In the anchorage-independent soft-agar assay, the colony numbers formed by ARH2-WT-transfected cells were much lower than that of vector or ARH2-Mut-transfected cells. The histogram shows the average numbers of colonies in each experiment. **D**, In the MTT assay, the growth rates of ARH2-Mut-transfected BPH-1 or P69 cells were significantly greater than that of vector transfected cells ( $P < 0.005$ ;  $t$  test). **E**, In the colony formation assay, the numbers of colonies in ARH2-Mut-transfected BPH-1 or P69 cells were much greater than that of vector-transfected cells.

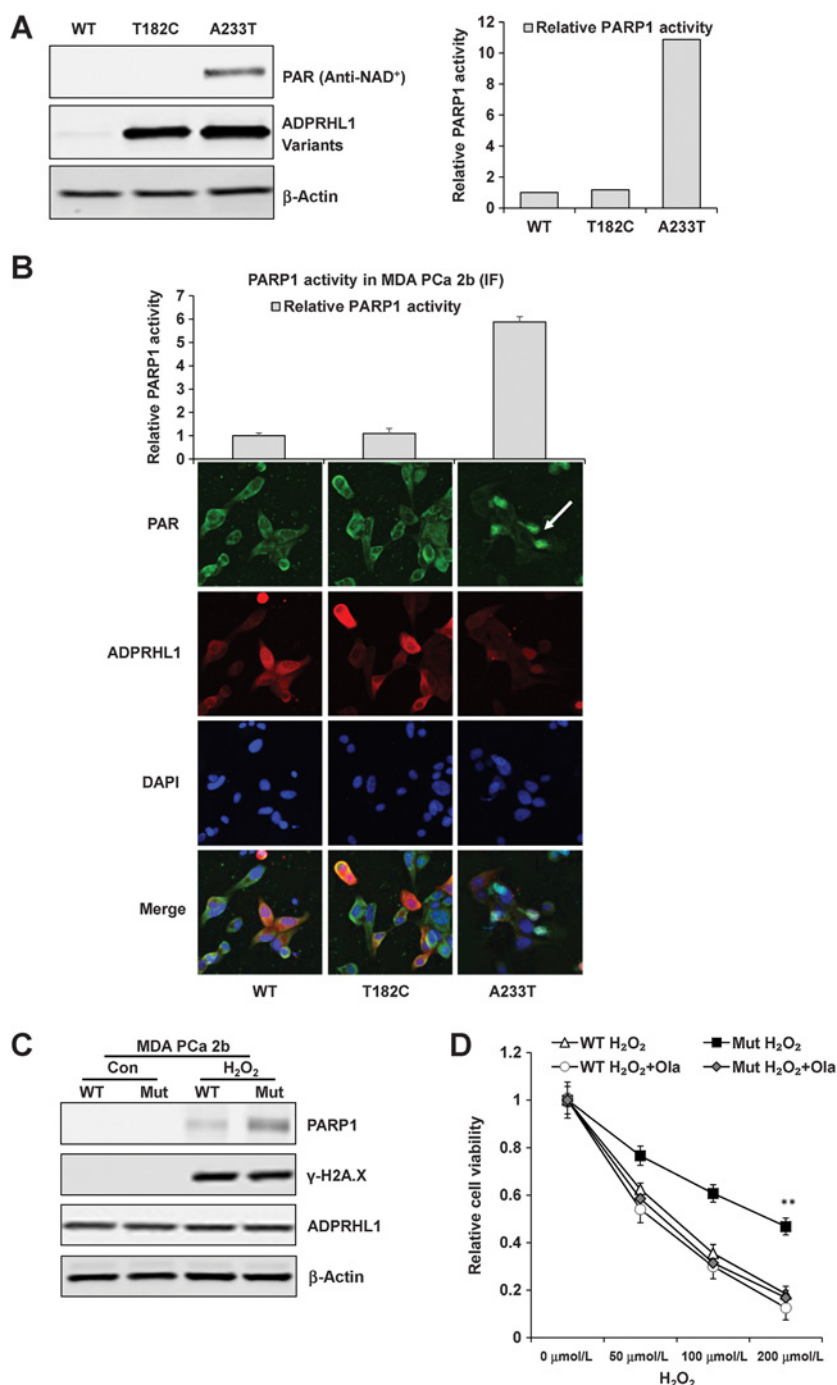
negative levels of ADPRHL1 in 19/20 (95%) of tumor tissues with Gleason scores of 8–10 based on their IHC staining scores (Fig. 4D). The detailed IHC scores of these samples are shown in Supplementary Table S2. Intriguingly, all four tumors in the Gleason 8–10 group with very weak levels of ADPRHL1 were all Gleason score 8 tumors, whereas the remaining 16 tumors in the same group with Gleason score of 9–10 were completely absent of ADPRHL1 expression. These data indicate that ADPRHL1 is significantly downregulated in prostate cancer and stepwise reduction of ADPRHL1 expression correlates with prostate cancer progression. Therefore, the potential tumor-suppressor ADPRHL1 is also very likely a potent biomarker for monitoring prostate cancer development and progression.

## Discussion

Here, we reported an AA-specific *ADPRHL1* germline mutation (*c.A233T*; *p.D78V*) that is associated with prostate cancer risk in hereditary AA-PC families. Although the carrier frequency of this mutation is about 25-fold higher in AA-PC families compared with the general AA population, the frequency of this germline mutation in healthy men based on the gnomAD database is relatively high ( $\sim 0.8\%$ ; [https://gnomad.broadinstitute.org/variant/13-114098886-T-A?dataset=gnomad\\_r2\\_1](https://gnomad.broadinstitute.org/variant/13-114098886-T-A?dataset=gnomad_r2_1)). Two factors may need to be considered in regards to this observation. First, prostate cancer is a late-onset disease. It is very likely that the relatively high frequency of this mutation in these high-risk families is due to high numbers of males recruited in the databases at younger ages

**Figure 3.**

ADPRHL1 mutation contributes to prostate cancer cell survival via activating PARP1-mediated DNA repair. **A**, In the *in vitro* PARP1 activity assay, the level of PAR was increased in ARH2-Mut-transfected MDA PCa 2b cells than that of ARH2-WT or Polymorphism-ARH2 (T182C) transfected cells. The  $\beta$ -actin was used as a loading control. The left histogram shows the relative PARP1 activities of WT-, Mut-, and Polymorphism-ARH2 transfected cells (**B**) In PARP1 *in vivo* immunofluorescence activity analyses, more PAR was accumulated in the nucleus of ARH2-Mut transfected cells (Arrow) than in WT- or Polymorphism-ARH2 transfected cells. The relative PARP1 activities of transfected cells with WT-, Mut- or Polymorphism-ARH2 are shown in the histogram on the top of the figure. **C**, Under the same DNA damage condition induced by 50  $\mu$ mol/L  $H_2O_2$ , PARP1 protein level showed higher in MDA PCa 2b cells transfected with ARH2-Mut than cells transfected with ARH2-WT. Two left lanes in the western blot were controls without DNA damage applied. **D**, Cell viability assay (MTT) of ARH2-Mut transfected MDA PCa 2b cells was significantly greater than ARH2-WT transfected cells under the same DNA damage condition induced by  $H_2O_2$ . However, the PARP1 inhibitor, olaparib, showed strong suppression of MDA PCa 2b cell viability and survival induced by ARH2-Mut.



(<50 years old), where the mutation is present but without any diagnosis or prostate cancer symptoms. It is evident that 40% of the individuals analyzed in the gnomAD dataset were below 50 years of age ([https://gnomad.broadinstitute.org/variant/13-114098886-T-A?dataset=gnomad\\_r2\\_1](https://gnomad.broadinstitute.org/variant/13-114098886-T-A?dataset=gnomad_r2_1)). Second, prostate cancer has the highest genetic inheritability among all solid tumors, and up to 10% of total prostate cancer cases are hereditary. Thus, the prostate cancer-associated mutation frequency in the general AA population could be well over 1% or even higher. In addition, an unaffected male from family #3 who was 47-years-old at the time

recruitment, with no prostate cancer symptoms, did carry this specific mutation (Fig. 1), which further supports that the mutation carriers below age 50 may generally not display prostate cancer symptoms. Therefore, further investigation of the ADPRHL1 mutation is warranted, not only in large numbers of high-risk AA-PC families, but also in large cohorts of AA healthy men who are 50 years or older.

ADPRHL1 (also known as ARH2) is one of the ARH family members (ARH1-3) that are ADP-ribose-acceptor hydrolases (27, 28). ARH protein performs ADP-ribosylation, a post-translational



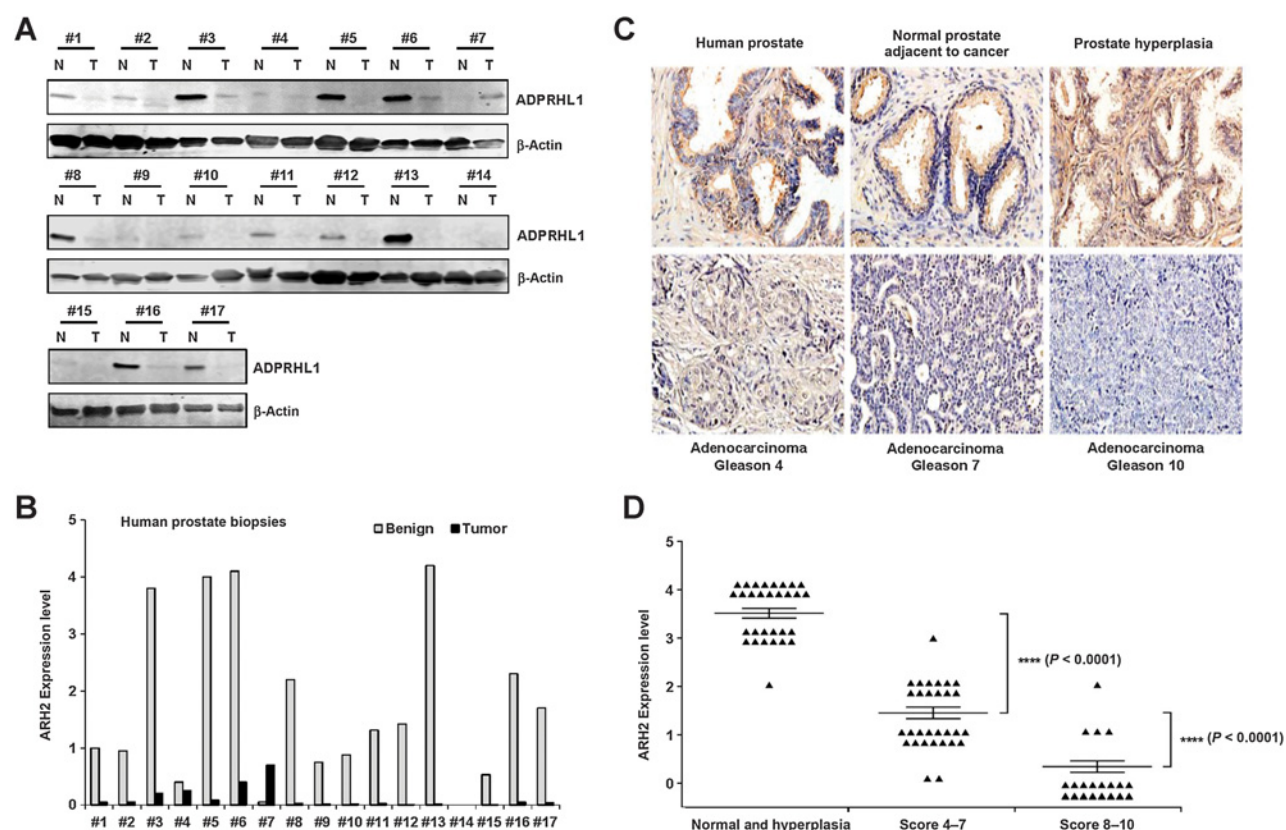


**Figure 4.**

ADPRHL1 is downregulated in prostate tumors. **A**, ADPRHL1 protein levels were determined in 17 pairs of prostate tumors and their matched adjacent normal prostate tissues by using Western blotting analyses.  $\beta$ -Actin was used as the loading control. **B**, The Western bands observed in (**A**) were quantified by using Image Studio Ver 3.1 of Odyssey CLx System (LICOR). **C**, Representative images of IHC for ADPRHL1 in the prostate tissue microarray (Catalog #PR807b) purchased from Biomax. The top three images represent IHC staining of ADPRHL1 in the normal prostate, the normal prostate tissue adjacent to cancer, and tissues with prostate hyperplasia as indicated. The three images below represent IHC staining of ADPRHL1 in the prostate adenocarcinoma tissues of Gleason score 4, 7, or 10, respectively (Magnifications, **C**:  $\times 400$ ). **D**, Stepwise correlation of ADPRHL1 expression levels and prostate cancer progression. Dot plots show that 29/30 normal or prostate hyperplasia tissues have the highest levels of ADPRHL1 (scored as +++ or ++++ in IHC staining), 27/30 prostate tumors with Gleason scores of 4-7 have mild levels of ADPRHL1 (scored as + and ++), and 19/20 tumors with Gleason scores of 8-10 have very weak or negative levels of ADPRHL1 (scored as + and -; Supplementary Table S2).

protein modification, to alter activities of targeted proteins (13). ARH1 controls mono-(ADP-ribosyl)ation to regulate cell proliferation and cancer suppression (29). *Arh1*<sup>-/-</sup> mice were cancer prone and developed carcinoma, lymphoma, and sarcoma in a variety of tissues except the prostate (30, 31). Interestingly, tumorigenesis seen in *Arh1*<sup>-/-</sup> mice is gender-specific; female mice developed tumors more frequently at a younger age than did male mice (32). *Arh3*<sup>-/-</sup> mice is embryonic lethal. Studies of *Arh3*<sup>-/-</sup> MEFs showed that Arh3 participates in the degradation of PAR (synthesized by PARP1) in response to oxidative stress-induced DNA damage, which leads to suppression of PAR-mediated cell death (24). To date, studies on ADPRHL1 are very limited. One study in *Xenopus* showed that Adprh1s was essential for heart chamber growth (33). The function of ADPRHL1 and its roles in cancer were unknown until this present study was performed. In this report, we demonstrated for the first time that ADPRHL1 regulates PARP1 activity in prostate leading to suppression of prostate cancer tumorigenesis and susceptibility.

PARP1 is a critical effector in prostate cancer development and therapy (34, 35). It is required for DNA repair, transcriptional regulation, cell-cycle control, metastasis and susceptibility of pros-

tate (36, 37). PARP1 activation was observed in the majority of prostate cancer tissues (38-40). However, the mechanisms for PARP1 deregulation in prostate cancer are not fully understood. We discovered and demonstrated that PARP1 is suppressed by ADPRHL1 in prostate. Mutation in *ADPRHL1* activates PARP1 leading to promotion of PARP1-mediated DNA repair capability in prostate cancer cells for cancer cell survival and tumorigenesis. Because downregulation of ADPRHL1 protein levels in prostate cancer tumor tissues is common, we speculate that in addition to the germline mutation we found in its coding region, regulatory variants in the 5' and 3' UTR regions and somatic mutations in *ADPRHL1* are probably also associated with ADPRHL1 downregulation and prostate cancer tumorigenesis.

In summary, we discovered the novel recurrent germline mutation *c.A233T* in the *ADPRHL1* gene in 4/20 of high-risk AA-prostate cancer families. Molecular and pathological analyses demonstrate that ADPRHL1 is a tumor suppressor and that the *c.A233T* mutation in this gene is oncogenic in prostate tissue by activation of PARP1 resulting in increasing DNA damage-induced DNA repair response to promote prostate cancer cell survival. We also demonstrate very significant clinical relevance of ADPRHL1 expression levels in prostate

cancer progression. These findings show that proper control of PARP1 protein levels affected by ADPRHL1 is essential for prostate cancer suppression and provide a new direction for developing ADPRHL1–PARP1 axis-based therapies to treat AA patients with prostate cancer with ADPRHL1 mutations. Future implications of ADPRHL1 mutations in prostate cancer risk assessment and new therapeutic applications may help to reduce prostate cancer mortality in the AA population.

### Authors' Disclosures

No disclosures were reported.

### Authors' Contributions

**G. Zhang:** Data curation, formal analysis, validation, investigation, visualization, methodology, writing—original draft. **Z. Wang:** Data curation, formal analysis, validation, investigation, methodology. **J. Bavarva:** Data curation, formal analysis, validation, investigation, methodology. **K.J. Kuhns:** Data curation, validation, investigation, writing—original draft. **J. Guo:** Conceptualization, investigation, methodology. **E.M. Ledet:** Resources, data curation, formal analysis, validation, investigation. **C. Qian:** Resources, data curation, formal analysis, validation, investigation. **Y. Lin:** Data curation, software, formal analysis, validation, investigation, methodology. **Z. Fang:** Conceptualization, data curation, software, formal analysis, investigation, methodology. **J. Zabaleta:** Data curation, software, formal analysis, validation, investigation, methodology. **L. Del Valle:** Data curation, formal analysis, validation,

investigation, visualization, methodology. **J.J. Hu:** Conceptualization, resources, validation, investigation, methodology. **D. Mandal:** Conceptualization, resources, data curation, formal analysis, supervision, validation. **W. Liu:** Conceptualization, resources, data curation, supervision, funding acquisition, validation, investigation, methodology, project administration, writing—review and editing.

### Acknowledgments

We thank the patients, the patients' family members, and the healthy individuals who participated in this research. We also thank Dr. Yan Dong (Tulane University) for providing cell lines and Susan C. Theodosiou for critical editing of this article. This work was supported by grants R21CA185213 and R21CA223119 from the National Institutes of Health (to W. Liu) and Louisiana Board of Regents [LEQSF (2002–05)–RD–A–15], the NCI (1R03CA097778), the Cancer Research Foundation of America, the Centers for Disease Control and Prevention (H57/CCH 624034–01; to D. Mandal).

The publication costs of this article were defrayed in part by the payment of publication fees. Therefore, and solely to indicate this fact, this article is hereby marked "advertisement" in accordance with 18 USC section 1734.

### Note

Supplementary data for this article are available at Molecular Cancer Research Online (<http://mcr.aacrjournals.org/>).

Received October 26, 2021; revised March 15, 2022; accepted July 5, 2022; published first July 11, 2022.

### References

- Bray F, Ren JS, Masuyer E, Ferlay J. Global estimates of cancer prevalence for 27 sites in the adult population in 2008. *Int J Cancer* 2013;132:1133–45.
- Lichtenstein P, Holm NV, Verkasalo PK, Iliadou A, Kaprio J, Koskenvuo M, et al. Environmental and heritable factors in the causation of cancer—analyses of cohorts of twins from Sweden, Denmark, and Finland. *N Engl J Med* 2000;343:78–85.
- Mucci LA, Hjelmborg JB, Harris JR, Czene K, Havelick DJ, Scheike T, et al. Nordic twin study of cancer (NorTwinCan) collaboration familial risk and heritability of cancer among twins in Nordic countries. *JAMA* 2016;315:68–76.
- Hemminki K. Genetic epidemiology—science and ethics on familial cancers. *Acta Oncol* 2001;40:439–44.
- Tonon L, Fromont G, Boyault S, Thomas E, Ferrari A, Sertier AS, et al. Mutational profile of aggressive, localised prostate cancer from african caribbean men versus european ancestry men. *Eur Urol* 2019;75:11–5.
- Attard G, Parker C, Eeles RA, Schroder F, Tomlins SA, Tannock I, et al. Prostate cancer. *Lancet* 2016;387:70–82.
- Frank C, Sundquist J, Hemminki A, Hemminki K. Familial associations between prostate cancer and other cancers. *Eur Urol* 2017;71:162–5.
- Petrovics G, Li H, Stumpel T, Tan SH, Young D, Katta S, et al. A novel genomic alteration of LSAMP associates with aggressive prostate cancer in African American men. *EBioMedicine* 2015;2:1957–64.
- Koboldt DC, Kanchi KL, Gui B, Larson DE, Fulton RS, Isaacs WB, et al. Rare variation in TET2 is associated with clinically relevant prostate carcinoma in African Americans. *Cancer Epidemiol Biomarkers Prev* 2016;25:1456–63.
- Huang FW, Mosquera JM, Garofalo A, Oh C, Baco M, Amin-Mansour A, et al. Exome sequencing of African-American prostate cancer reveals loss-of-function ERF mutations. *Cancer Discov* 2017;7:973–83.
- Jaratlerdsiri W, Chan EKF, Gong T, Petersen DC, Kalsbeek AMF, Venter PA, et al. Whole-genome sequencing reveals elevated tumor mutational burden and initiating driver mutations in African men with treatment-naive, high-risk prostate cancer. *Cancer Res* 2018;78:6736–46.
- Mandal DM, Sartor O, Halton SL, Mercante DE, Bailey-Wilson JE, Rayford W. Recruitment strategies and comparison of prostate cancer-specific clinical data on African-American and Caucasian males with and without family history. *Prostate Cancer Prostatic Dis* 2008;11:274–9.
- Ledet EM, Sartor O, Rayford W, Bailey-Wilson JE, Mandal DM. Suggestive evidence of linkage identified at chromosomes 12q24 and 2p16 in African American prostate cancer families from Louisiana. *Prostate* 2012;72:938–47.
- Haiman CA, Chen GK, Blot WJ, Strom SS, Berndt SI, Kittles RA, et al. Genome-wide association study of prostate cancer in men of African ancestry identifies a susceptibility locus at 17q21. *Nat Genet* 2011;43:570–3.
- Wang Z, Wang Z, Guo J, Li Y, Bavarva JH, Qian C, et al. Inactivation of androgen-induced regulator ARD1 inhibits androgen receptor acetylation and prostate tumorigenesis. *Proc Natl Acad Sci U S A* 2012;109:3053–8.
- Reddy A, Espinoza I, Cole D, Schallheim J, Poosarla T, et al. Genetic mutations in B-acute lymphoblastic leukemia among African American and European American children. *Clin Lymphoma Myeloma Leuk* 2018;18:e501–8.
- Choi M, Scholl UI, Ji W, Liu T, Tikhonova IR, Zumbo P, et al. Genetic diagnosis by whole exome capture and massively parallel DNA sequencing. *Proc Natl Acad Sci USA* 2009;106:19096–101.
- Li H, Handsaker B, Wysoker A, Fennell T, Ruan J, Homer N, et al. 1000 genome project data processing subgroup. The sequence alignment/map (SAM) format and SAM tools. *Bioinformatics* 2009;25:2078–9.
- Bilguvar K, Tyagi NK, Ozkara C, Tuysuz B, Bakircioglu M, Choi M. Recessive loss of function of the neuronal ubiquitin hydrolase UCHL1 leads to early-onset progressive neurodegeneration. *Proc Natl Acad Sci USA* 2013;110:3489–94.
- Itan Y, Shang L, Boisson B, Ciancanelli MJ, Markle JG, Martinez-Barricarte R, et al. The mutation significance cutoff: gene-level thresholds for variant predictions. *Nat Methods* 2016;13:109–10.
- Zhang G, Liu X, Li J, Ledet E, Alvarez X, Qi Y, et al. Androgen receptor splice variants circumvent AR blockade by microtubule-targeting agents. *Oncotarget* 2015;6:23358–71.
- Zhan Y, Zhang G, Wang X, Qi Y, Bai S, Li D, et al. Interplay between cytoplasmic and nuclear androgen receptor splice variants mediates castration resistance. *Mol Cancer Res* 2017;15:59–68.
- Ewing CM, Ray AM, Lange EM, Zuhlke KA, Robbins CM, Tembe WD, et al. Germline mutations in HOXB13 and prostate-cancer risk. *N Engl J Med* 2012;366:141–9.
- Mashimo M, Kato J, Moss J. ADP-ribosyl-acceptor hydrolase 3 regulates poly (ADP-ribose) degradation and cell death during oxidative stress. *Proc Natl Acad Sci U S A* 2013;110:18964–9.
- Bu X, Kato J, Moss J. Emerging roles of ADP-ribosyl-acceptor hydrolases (ARHs) in tumorigenesis and cell death pathways. *Biochem Pharmacol* 2019;167:44–9.
- Krietsch J, Caron MC, Gagné JP, Ethier C, Vignard J, Vincent M, et al. PARP activation regulates the RNA-binding protein NONO in the DNA damage response to DNA double-strand breaks. *Nucleic Acids Res* 2012;40:10287–301.
- Mashimo M, Kato J, Moss J. Structure and function of the ARH family of ADP-ribosyl-acceptor hydrolases. *DNA Repair* 2014;23:88–94.



28. Mashimo M, Moss J. ADP-Ribosyl-acceptor hydrolase activities catalyzed by the ARH family of proteins. *Methods Mol Biol* 2018;1813:187–204.
29. Kato J, Zhu J, Liu C, Stylianou M, Hoffmann V, Lizak MJ, et al. ADP-ribosylarginine hydrolase regulates cell proliferation and tumorigenesis. *Cancer Res* 2011;71:5327–35.
30. Kato J, Vekhter D, Heath J, Zhu J, Barbieri JT, Moss J. Mutations of the functional ARH1 allele in tumors from ARH1 heterozygous mice and cells affect ARH1 catalytic activity, cell proliferation, and tumorigenesis. *Oncogenesis* 2015;4:e151.
31. H Ishiwata-Endo K J, Stevens LA, Moss J. ARH1 in health and disease. *Cancers* 2020;12:479.
32. Watanabe K, Kato J, Zhu J, Oda H, Ishiwata-Endo H, Moss J. Enhanced sensitivity to cholera toxin in female ADP-ribosylarginine hydrolase (ARH1)-deficient mice. *PLoS One* 2018;13:e0207693.
33. Smith SJ, Towers N, Saldanha JW, Shang CA, Mahmood SR, Taylor WR, et al. The cardiac-restricted protein ADP-ribosylhydrolase-like 1 is essential for heart chamber outgrowth and acts on muscle actin filament assembly. *Dev Biol* 2016; 416:373–88.
34. Deshmukh D, Qiu Y. Role of PARP-1 in prostate cancer. *Am J Clin Exp Urol* 2015;3:1–12.
35. Schiewer MJ, Goodwin JF, Han S, Brenner JC, Augello MA, Dean JL, et al. Dual roles of PARP-1 promote cancer growth and progression. *Cancer Discov* 2012;2: 1134–49.
36. Chaudhuri AR, Nussenzweig A. The multifaceted roles of PARP1 in DNA repair and chromatin remodelling. *Nat Rev Mol Cell Biol* 2017;18:610–21.
37. Rouleau M, Patel A, Hendzel MJ, Kaufmann SH, Poirier GG. PARP inhibition: PARP1 and beyond. *Nat Rev Cancer* 2010;10:293–301.
38. Li N, Chen J. ADP-ribosylation: activation, recognition, and removal. *Mol Cells* 2014;37:9–16.
39. Salemi M, Galia A, Frassetta F, La Corte C, Pepe P, La Vignera S, et al. Poly (ADP-ribose) polymerase 1 protein expression in normal and neoplastic prostatic tissue. *Eur J Histochem* 2013;57:e13.
40. Wu W, Zhu H, Liang Y, Kong Z, Duan X, Li S, et al. Expression of PARP-1 and its active polymer PAR in prostate cancer and benign prostatic hyperplasia in Chinese patients. *Int Urol Nephrol* 2014;46:1345–9.